Biochemical and Biophysical Research Communications 439 (2013) 270–274

Contents lists available at ScienceDirect

Biochemical and Biophysical Research Communications

journal homepage: www.elsevier.com/locate/ybbrc

Potent inhibition of L-type Ca^{2+} currents by a Rad variant associated with congestive heart failure

U. Meza [a,b,*], D. Beqollari [a], C.F. Romberg [a], S. Papadopoulos [c], R.A. Bannister [a,*]

[a] Department of Medicine-Cardiology Division, University of Colorado Denver-Anschutz Medical Campus, 12700 East 19th Avenue, P15-8006, B-139, Aurora, CO 80045, USA
[b] Departamento de Fisiología y Biofísica, Facultad de Medicina, Universidad Autónoma de San Luis Potosí, Venustiano Carranza #2405, San Luis Potosí, SLP 78210, México
[c] Department of Vegetative Physiology, University of Cologne, Robert-Koch-Str. 39, D-50931 Cologne, Germany

ARTICLE INFO

Article history:
Received 11 August 2013
Available online 20 August 2013

Keywords:
Rad
RGK protein
$Ca_V1.2$
$Ca_V1.3$
L-type
Heart failure

ABSTRACT

Ca^{2+} influx via L-type voltage-gated Ca^{2+} channels supports the plateau phase of ventricular action potentials and is the trigger for excitation–contraction (EC) coupling in the myocardium. Rad, a member of the RGK (Rem, Rem2, Rad, Gem/Kir) family of monomeric G proteins, regulates ventricular action potential duration and EC coupling gain through its ability to inhibit cardiac L-type channel activity. In this study, we have investigated the potential dysfunction of a naturally occurring Rad variant (Q66P) that has been associated with congestive heart failure in humans. Specifically, we have tested whether Rad Q66P limits, or even eliminates, the inhibitory actions of Rad on $Ca_V1.2$ and $Ca_V1.3$, the two L-type channel isoforms known to be expressed in the heart. We have found that mouse Rad Q65P (the murine equivalent of human Rad Q66P) inhibits L-type currents conducted by $Ca_V1.2$ or $Ca_V1.3$ channels as potently as wild-type Rad (>95% inhibition of both channels). In addition, Rad Q65P attenuates the gating movement of both channels as effectively as wild-type Rad, indicating that the Q65P substitution does not differentially impair any of the three described modes of L-type channel inhibition by RGK proteins. Thus, we conclude that if Rad Q66P contributes to cardiomyopathy, it does so via a mechanism that is not related to its ability to inhibit L-type channel-dependent processes *per se*. However, our results do not rule out the possibility that decreased expression, mistargeting or altered regulation of Rad Q66P may reduce the RGK protein's efficacy *in vivo*.

1. Introduction

In the heart, Ca^{2+} influx via L-type voltage-gated Ca^{2+} channels ($Ca_V1.2$) forms the electrophysiological basis for the plateau phase of action potentials and triggers the Ca^{2+} release from the sarcoplasmic reticulum (SR) necessary for contracture of the myocardium [1,2]. Since L-type channel activity is absolutely essential for maintaining rhythm and for excitation–contraction (EC) coupling, modulators of L-type channel activity can have profound effects on cardiac physiology. In this regard, members of the RGK (Rem, Rem2, Rad, Gem/Kir) family of small Ras-related GTP-binding proteins are potent endogenous inhibitors of both $Ca_V1.2$, the predominant cardiac L-type isoform, and $Ca_V1.3$, which is highly expressed in the sinoatrial node [3–12], reviewed in [13]. In acutely isolated cardiomyocytes and in cultured cardiac cells, viral overexpression of Gem, Rem or Rad substantially reduces L-type currents [5–9,12], dampens EC coupling [6,8,9] and shortens the plateau phase of ventricular action potentials [5,7,8]. The attenuation of L-type channel activity by Rad, Rem or Gem *in vitro* correlates with shortened QT intervals [5,7] and decreased left ventricular systolic pressure *in vivo* [5]. Overexpression of Rad or Rem also prevents β-adrenergic enhancement of native L-type current and the consequential extension of the plateau phase of the action potential [7,8].

Suppression of RGK protein activity can also profoundly affect cardiac function. For example, Yada and colleagues [7] observed increased L-type current, broadened action potentials and prolonged QT intervals in an engineered mouse overexpressing a putative dominant-negative form of Rad (S105N). The prolongation of the QT interval in the transgenic Rad S105N mice produced a variety of arrhythmias including sinus node dysfunction, atrioventricular block and ventricular extra systoles. Moreover, administration of the β-adrenergic agonist epinephrine induced ventricular tachycardia. Along the same lines, Wang et al. [9] reported that L-type currents and EC coupling were augmented in dissociated ven-

Abbreviations: EC, excitation–contraction; RGK, Rad-Rem-Rem2-Gem/Kir protein; RyR2, type 2 ryanodine-sensitive intracellular Ca^{2+} release channel; SR, sarcoplasmic reticulum.

* Corresponding authors. Address: Department of Medicine-Cardiology Division, University of Colorado Denver-Anschutz Medical Campus, 12700 East 19th Avenue, P15-8006, B-139, Aurora, CO 80045, USA. Fax: +1 (303) 724 5450 (U. Meza, R.A. Bannister).

E-mail addresses: umeza@uaslp.mx (U. Meza), donald.beqollari@ucdenver.edu (D. Beqollari), christin.romberg@ucdenver.edu (C.F. Romberg), spapadop@uni-koeln.de (S. Papadopoulos), roger.bannister@ucdenver.edu (R.A. Bannister).

0006-291X/$ - see front matter © 2013 Elsevier Inc. All rights reserved.
http://dx.doi.org/10.1016/j.bbrc.2013.08.044

tricular myocytes infected with siRNA directed against Rad. Somewhat surprisingly, EC coupling was found to be blunted in cardiomyocytes harvested from Rem null mice, even though L-type current was modestly enhanced and SR Ca^{2+} stores were replete [14].

Rad has been identified as a negative regulator of cardiac hypertrophy in a study showing that: (1) heart failure patients have decreased levels of Rad message and expressed protein, (2) overexpression of Rad blocks the hypertrophic response in phenylephrine-treated cultured neonatal cardiomyocytes, and (3) mice lacking Rad are more susceptible to the development of hypertrophy in response to thoracic transverse aortic constriction than wild-type mice [15]. Interestingly, a thymine to guanine switch at Rad bp 2248 encoding a glutamine to proline swap at Rad residue 66 has been identified in congestive heart failure patients by a group of investigators aiming to profile nonsynonymous single nucleotide polymorphisms in known signaling proteins [16].

Taken together, the earlier observations that L-type Ca^{2+} flux [17] and genetic ablation of Rad [15] both promote pathological cardiac hypertrophy raise the question of whether aberrant Ca^{2+} influx via L-type channels resulting from impaired Rad Q66P function may play a role in the pathogenesis of some forms of heart failure. To investigate this idea at the most basic level, we have tested the ability of this Rad variant to inhibit L-type Ca^{2+} currents conducted by $Ca_V1.2$ and $Ca_V1.3$ channels.

2. Materials and methods

2.1. Molecular biology

The cDNA plasmid encoding Venus-mouse Rad (GenBank accession No. NP_062636) was a kind gift from Drs. S.R. Ikeda and H.J. Puhl, III (NIH/NIAAA). The missense mutation encoding a glutamine to proline swap at mouse Rad residue 65 was introduced into the V-Rad parent vector using the Change-IT site directed mutagenesis kit (cat. #784801KT; Affymetrix, Santa Clara, CA). The sequence of the forward primer was 5′-GAACTCGGACACcGGGCCAGAGG-3′ and the sequence of the reverse primer was 5′-CTCCATCCACAGTGATAGAACGGTC-3′. The presence of the mutation was verified by sequencing.

2.2. tsA201 cell culture and expression of cDNA

tsA201 cells were propagated in culture medium containing 90% DMEM (cat. #SH30022.01; HyClone Thermo Scientific, Logan, UT), 10% defined fetal bovine serum (Hyclone Laboratories) and 100 μg/ml Penicillin–Streptomycin (cat. #15140-122; Life Technologies, Grand Island, NY). tsA201cells of low passage number (<20) were trypsinized twice weekly and replated onto 35 mm culture dishes at ~20% confluence. Lipofectamine 2000 (cat. #11668-019; Life Technologies, Carlsbad, CA) was used to transfect these cells within 3–5 days of plating. The transfection mixture contained expression plasmids encoding rabbit $Ca_V1.2$ [18] or rat $Ca_V1.3$ [19], rat $\alpha_2\delta1$ [20] and rabbit β_{2a} [21] channel subunits at 1 μg of each cDNA per dish. Where appropriate, the transfection mixture contained a plasmid-encoding mouse Venus-Rad (1 μg/dish), mouse Venus-Rad Q65P (1 μg/dish) or YFP (30 ng/dish; Clontech, Mountain View, CA). The day following transfection, cells were trypsinized and replated onto 35 mm plastic culture dishes (BD Falcon, San Jose, CA; cat. #353801). Cells were used in recording experiments ~24 h later.

2.3. Measurement of L-type Ca^{2+} currents and intramembrane charge movements

All experiments were performed at room temperature (~25 °C). Pipettes (2.0–3.0 MΩ) were fabricated from borosilicate glass and were filled with internal solution, which consisted of (in mM): 140 Cs-aspartate, 10 Cs_2-EGTA, 5 $MgCl_2$ and 10 HEPES, pH 7.4 with CsOH. The bath solution contained: 145 NaCl, 10 $CaCl_2$ and 10 HEPES, pH 7.4 with NaOH. For measurement of intramembrane charge movements attributable to $Ca_V1.2$, 0.1 $LaCl_3$ and 0.5 $CdCl_2$ were added to the bath solution. Electronic compensation was used to reduce the effective series resistance. Linear components of leak and capacitive current were corrected with $-P/4$ online subtraction protocols. Filtering was at 2–5 kHz and digitization was either at 10 kHz (L-type currents) or 25 kHz (charge movements). Cell capacitance was determined by integration of a transient from −80 to −70 mV using Clampex 10.3 (Molecular Devices, Sunnyvale, CA) and was used to normalize charge movements (fC/pF) and current amplitudes (pA/pF). Current–voltage (I–V) curves were fitted according to:

$$I = G_{max}(V - V_{rev})/\{1 + \exp[-(V - V_{1/2})/k_G]\} \quad (1)$$

where I is the normalized current for the test potential V, V_{rev} is the reversal potential, G_{max} is the maximum conductance, $V_{1/2}$ is the half-maximal activation potential and k_G is the slope factor. For $Ca_V1.2$, plots of the integral of the ON charge movement (Q_{on}) as a function of test potential (V) were fitted according to:

$$Q_{on} = Q_{max}/\{1 + \exp[(V - V_Q)/k_Q]\}, \quad (2)$$

where Q_{max} is the maximal Q_{on}, V_Q is the potential causing movement of half the maximal charge, and k_Q is a slope parameter. Since Cd^{2+} and La^{3+} failed to adequately block L-type current conducted by $Ca_V1.3$, integration of the ON charges movement at the reversal potential was employed to determine Q_{max}.

2.4. Analysis

Figures were made using the software program SigmaPlot (version 11.0, SSPS Inc., San Jose, CA). Data are presented as mean ± SEM. Statistical comparisons were made by unpaired t-test or by *ANOVA* (where appropriate) with $P < 0.05$ considered significant.

3. Results

3.1. Rad Q65P potently inhibits $Ca_V1.2$ channels

To determine whether the Rad Q66P polymorphism (please see Fig. 1) impairs the small G protein's ability to inhibit $Ca_V1.2$, we recorded L-type currents from transiently transfected tsA201cells. In control experiments, we observed robust L-type currents in tsA201cells expressing $Ca_V1.2$, auxiliary β_{2a} and $\alpha_2\delta1$ subunits and a YFP transfection marker (−18.7 ± 2.7 pA/pF at +20 mV, $n = 15$; Fig. 2A and D). As expected, coexpression of a Venus-fused wild-type Rad construct nearly ablated (>95% reduction) any current attributable to $Ca_V1.2$ (−0.1 ± 0.4 pA/pF, $n = 15$; Fig. 2B and D). Similarly, L-type currents were also nearly eliminated by coexpression of V-Rad Q65P, the murine equivalent of human Rad Q66P (−0.4 ± 0.5 pA/pF, $n = 15$; $P > 0.05$, unpaired t-test *vs.* V-Rad; Fig. 2C

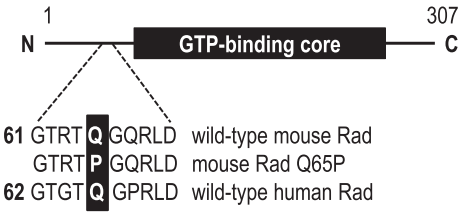

Fig. 1. Schematic diagram of the human Rad Q66P/mouse Rad Q65P substitution.

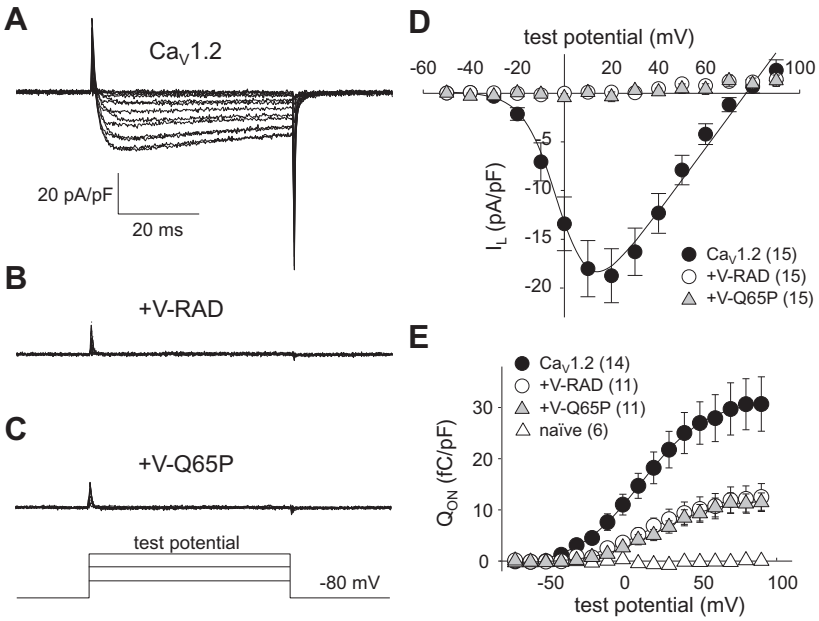

Fig. 2. Rad Q65P potently inhibits $Ca_V1.2$ channels expressed in tsA201cells. Representative recordings of L-type currents are shown for tsA201cells expressing $Ca_V1.2$, β_{2a}, $\alpha_2\delta1$, and YFP (A), $Ca_V1.2$, β_{2a}, $\alpha_2\delta1$, and V-Rad (B) and $Ca_V1.2$, β_{2a}, $\alpha_2\delta1$, and V-Rad Q65P (C). Currents were evoked at 0.1 Hz by 50 ms steps from −80 mV to test potentials ranging from −50 to +90 mV in 10 mV increments (illustrated at bottom of panel C). The peak *I–V* relationships are shown in (D). The smooth curve for the $Ca_V1.2$ control data set is plotted according to Eq. (1) with fit parameters: G_{max} = 358 ± 40 pS/pF, $V_{1/2}$ = −2.7 ± 2.3 mV and k_G = 8.3 ± 0.6 mV; the *I–V* relationships for V-Rad- and V-Rad Q65P-expressing cells were not able to be fit by Eq. (1). (E) Q-V relationships. Charge movements were evoked at 0.1 Hz by 25 ms steps from −80 mV to potentials ranging from −70 mV through +90 mV in 10 mV increments. The smooth curves are plotted according to Eq. (2) with fit parameters displayed in Table 1. Throughout, error bars represent ± SEM.

and D). No inward current was detectable in seven non-transfected tsA201 cells (data not shown).

RGK proteins inhibit L-type channels via three distinct mechanisms: (1) decreased channel membrane expression, (2) voltage-sensor immobilization and (3) reduced channel P_o [10,11,13]. Since the first two modes are characterized by impaired voltage-sensor function, we measured maximal ON charge movement to determine whether the Rad Q66P variant selectively impedes a particular inhibitory mode. As summarized in Fig. 2E, we observed a reduction in maximal charge movement that was nearly identical for cells expressing either V-Rad (12.9 ± 2.7 fC/pF, n = 11) or V-Rad Q65P (11.9 ± 2.0 fC/pF, n = 11; P > 0.05, unpaired *t*-test *vs.* V-Rad) relative to control cells (32.5 ± 4.8 fC/pF, n = 14; P < 0.001, *ANOVA*; see Table 1). Importantly, negligible charge movement was observed in non-transfected tsA201cells (0.01 ± 0.20 fC/pF; n = 6). Taken together, the results shown in Fig. 2 demonstrate that Rad Q65P inhibits $Ca_V1.2$ channels as potently as wild-type Rad by the same mode of action.

3.2. Rad Q65P also produces profound inhibition of $Ca_V1.3$ channels

We next examined the ability of Rad Q65P to inhibit $Ca_V1.3$ channels because this L-type channel isoform is also expressed in the heart [22,23]. Specifically, $Ca_V1.3$ expression is abundant in the sinoatrial node where it supports the upstroke of spontaneous action potentials and may play a key role in pacemaking [24–28]. In the control experiments shown in Fig. 3A, tsA201cells transfected with $Ca_V1.3$, β_{2a}, $\alpha_{2\delta}1$ subunits and YFP produced L-type currents that were much larger in amplitude (−155.4 ± 21.4 pA/pF at −10 mV, n = 26) and activated at more hyperpolarizing potentials than the $Ca_V1.2$ currents shown in Fig. 2A. However, the inhibitory effects of V-Rad and V-Rad Q65P coexpression on $Ca_V1.3$ channels were quite similar to those observed with the $Ca_V1.2$ isoform (Fig. 3B and C, compare with Fig. 2B and C); V-Rad and V-Rad Q65P both reduced $Ca_V1.3$ current by >95% (−3.0 ± 0.7 pA/pF, n = 13 and −3.1 ± 0.6 pA/pF, n = 20, respectively; P > 0.05, unpaired *t*-test; Fig. 2D). Likewise, the Q65P substitution had no significant effect on the reduction of $Ca_V1.3$ charge movement compared to wild-type Rad (7.1 ± 1.4 fC/pF, n = 20 and 4.2 ± 1.2 pA/pF, n = 13, respectively; P > 0.05, unpaired *t*-test; Fig. 3E). Thus, our data indicate that wild-type Rad and Rad Q65P inhibit both L-type channel isoforms known to be expressed in the heart to an equal extent.

Table 1
Q–V fit parameters.

	Q–V		
	Q_{max} (fC/pF)	V_Q (mV)	k_Q (mV)
$Ca_V1.2$	32.5 ± 4.8[a] (14)	18.1 ± 3.8	20.0 ± 1.5
$Ca_V1.2$ + V-Rad	12.9 ± 2.7 (11)	19.0 ± 5.9	18.5 ± 1.8
$Ca_V1.2$ + V-Rad Q65P	11.9 ± 2.0 (11)	23.9 ± 3.4	17.0 ± 0.9

Data are given as mean ± SEM, with the numbers in parentheses indicating the number of cells tested. Charge movement data were fit by Eq. (2). Significant differences are indicated.
[a] P < 0.001; *ANOVA*.

4. Discussion

Residue Q66 lies in the amino-terminus of human Rad, upstream of the GTP-binding core region (Fig. 1) [29,30]. We find that Rad Q66P (mouse Rad Q65P), a less common variant identified in a cohort of congestive heart failure patients, inhibits Ca^{2+} currents conducted by cardiac L-type channels ($Ca_V1.2$ and $Ca_V1.3$) as effectively as wild-type Rad (Figs. 2 and 3). Our results are consistent with the findings of earlier structure–function studies demonstrating that the less conserved amino-termini of RGK proteins are largely dispensable for inhibition of cloned high voltage-activated Ca^{2+} channels. In particular, RGK proteins minimally require an intact and membrane-targeted core to produce inhibition of Ca^{2+} channels in heterologous systems [31–33].

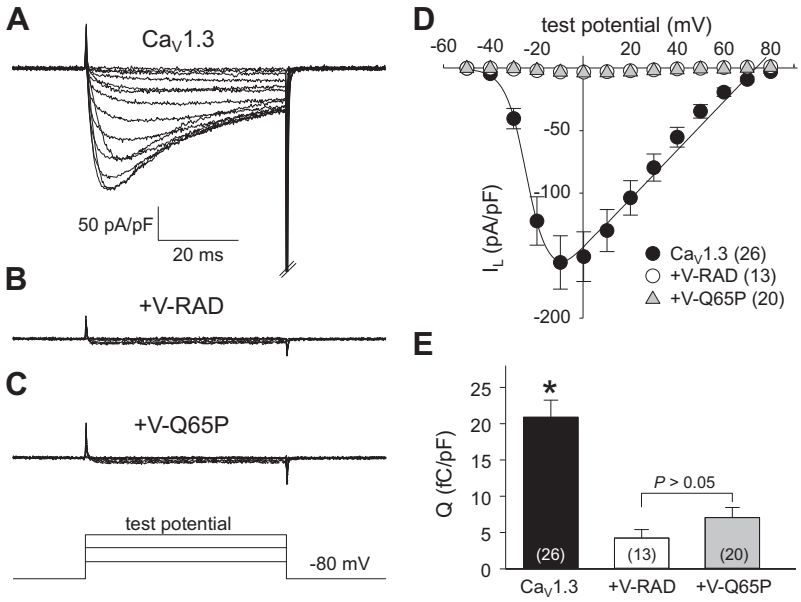

Fig. 3. Rad Q65P potently inhibits $Ca_V1.3$ channels expressed in tsA201cells. Representative recordings of L-type currents are shown for tsA201cells expressing $Ca_V1.3$, β_{2a}, $\alpha_2\delta1$, and YFP (A), $Ca_V1.3$, β_{2a}, $\alpha_2\delta1$, and V-Rad (B) and $Ca_V1.3$, β_{2a}, $\alpha_2\delta1$, and V-Rad Q65P (C). Currents were evoked at 0.1 Hz by 50 ms steps from −80 mV to depolarizations ranging from −50 to +80 mV in 10 mV increments. The peak *I–V* relationships are shown in (D). The smooth curve for the $Ca_V1.3$ control data set is plotted according to Eq. (1) with fit parameters: G_{max} = 1894 ± 228 pS/pF, $V_{1/2}$ = −23.2 ± 1.0 mV and k_G = 4.3 ± 0.2 mV. Again, the *I–V* relationships for V-Rad- and V-Rad Q65P-expressing cells were not able to be fit by Eq. (1). (E) Summary of average maximal charge movement. Since $Ca_V1.3$ Ca^{2+} currents were not completely blocked by Cd^{2+} and La^{3+}, Q_{max} was determined by integration of the "ON" charge elicited by step depolarizations from −80 mV to the reversal potential.

For both $Ca_V1.2$ and $Ca_V1.3$, a portion of intramembrane charge movement was preserved in cells expressing either wild-type Rad or Rad Q65P despite the near ablation of the Ca^{2+} current. By contrast, previous work has shown that overexpression of Rem nearly eliminates charge movement arising from $Ca_V1.2$ channels expressed in HEK293 cells [11]. Thus, Rad seems to rely more heavily on the low P_o voltage-sensor-mobile mode of RGK protein action in this cell type than does Rem. Moreover, we find that the reductions of maximal charge movement mediated by wild-type Rad and Rad Q65P are similar (Fig. 2E and Fig. 3E), indicating that neither the low P_o mode nor the two inhibitory modes that are characterized by reduced charge movement (i.e., enhanced channel internalization and voltage-sensor immobilization) are differentially affected by the Q65P substitution.

Taken together, our results appear to indicate that if Rad Q66P contributes to the development of cardiac hypertrophy and heart failure, it does so by interfering with a process that is not dependent on the intrinsic ability of the RGK protein to inhibit L-type Ca^{2+} channels. However, the Q66P substitution still may impair the effect of Rad on L-type channel activity *in vivo*. For example, a reduction in Rad Q66P expression may occur in human failing hearts even though Rad Q65P expression is similar to wild-type Rad in our heterologous expression system. Another potential mechanism for Rad Q66P dysfunction is that the introduction of a proline "kink" causes structural rearrangements within the amino-terminus that are detrimental to targeting or regulation of Rad activity. In regard the former, the amino-termini of RGK proteins house elements necessary for interactions with scaffolding proteins such as 14-3-3 which may anchor RGK proteins in close proximity to L-type channels [34]. Relevant to the latter possibility, one may speculate that the presence of a proline at residue 66 impedes regulatory events that stabilize Rad function (e.g., phosphorylation, acetylation, oxidation–reduction). Finally, a molecular mechanism by which the Rad Q66P polymorphism contributes to heart failure independently of Ca^{2+} channel modulation must be considered since RGK proteins are known regulators of the cytoskeleton, cell growth and metabolism [35–39]. In particular, the disruption of a channel-independent function may be involved the development of some forms of cardiomyopathy because Rad activity promotes apoptosis [40] and provides defence against heart failure by limiting fibrosis [41].

Acknowledgments

We thank Drs. S.R. Ikeda and H.L. Puhl III for sharing the Venus-Rad expression plasmid, Mr. M.P. Scheele for technical assistance and Dr. K.G. Beam for continued support. This work was supported by grants from the National Institutes of Health (AG038778 to R.A.B.), by startup funding from the University of Colorado Denver-AMC Department of Medicine-Cardiology Division and from CONACyT (169006 to U.M.). D.B. received a stipend from NIH/NIA 2T32AG000279-11 (to R.S. Schwartz, University of Colorado Denver-AMC Department of Medicine-Geriatrics Division).

References

[1] D.M. Bers, Calcium cycling and signaling in cardiac myocytes, Ann. Rev. Physiol. 70 (2008) 23–49.
[2] E. Marbán, Cardiac channelopathies, Nature 415 (2002) 213–218.
[3] P. Béguin, K. Nagashima, T. Gonoi, T. Shibasaki, K. Takahashi, Y. Kashima, N. Ozaki, K. Geering, T. Iwanaga, S. Seino, Regulation of Ca^{2+} channel expression at the cell surface by the small G-protein kir/Gem, Nature 411 (2001) 701–706.
[4] B.S. Finlin, S.M. Crump, J. Satin, D.A. Andres, Regulation of voltage-gated calcium channel activity by the Rem and Rad GTPases, Proc. Natl. Acad. Sci. USA 100 (2003) 14469–14474.
[5] M. Murata, E. Cingolani, A.D. McDonald, K. Donahue, E. Marbán, Creation of a genetic calcium channel blocker by targeted Gem gene transfer in the heart, Circ. Res. 95 (2004) 398–405.
[6] S.M. Crump, R.N. Correll, E.A. Schroder, W.C. Lester, B.S. Finlin, J. Satin, D.A. Andres, L-type calcium channel α-subunit and protein kinase inhibitors modulate Rem-mediated regulation of current, Am. J. Physiol. 291 (2006) H1959–H1971.
[7] H. Yada, M. Murata, K. Shimoda, S. Yuasa, H. Kawaguchi, M. Ieda, T. Adachi, S. Ogawa, K. Fukuda, Dominant negative suppression of Rad leads to QT prolongation and causes ventricular arrhythmias via modulation of L-type Ca^{2+} channels in the heart, Circ. Res. 101 (2007) 69–77.
[8] X. Xu, S.O. Marx, H.M. Colecraft, Molecular mechanisms, and selective pharmacological rescue, of Rem-inhibited $Ca_V1.2$ channels in heart, Circ. Res. 107 (2010) 620–630.

[9] G. Wang, X. Zhu, W. Xie, P. Han, K. Li, Z. Sun, Y. Wang, C. Chen, R. Song, C. Cao, J. Zhang, C. Wu, J. Liu, H. Cheng, Rad as a novel regulator of excitation–contraction coupling and β-adrenergic signaling in heart, Circ. Res. 106 (2010) 317–327.
[10] T. Yang, X. Xu, T. Kernan, V. Wu, H.M. Colecraft, Rem, a member of the RGK GTPases, inhibits recombinant $Ca_V1.2$ channels using multiple mechanisms that require distinct conformations of the GTPase, J. Physiol. 588 (2010) 1665–1668.
[11] T. Yang, A. Puckerin, H.M. Colecraft, Distinct RGK GTPases differentially use α_1- and auxiliary β-binding-dependent mechanisms to inhibit $Ca_V1.2/Ca_V2.2$ channels, PLoS One 7 (2012) e37079.
[12] B.S. Jhun, J. O-Uchi, W. Wang, C.H. Ha, J. Zhao, J.Y. Kim, C. Wong, R.T. Dirksen, C.M. Lopes, Z.G. Jin, Adrenergic signaling controls RGK-dependent trafficking of cardiac voltage-gated L-type Ca^{2+} channels through PKD1, Circ. Res. 110 (2012) 59–70.
[13] T. Yang, H.M. Colecraft, Regulation of voltage-dependent calcium channels by RGK proteins, Biochim. Biophys. Acta-Biomembr. 2013 (1828) 1644–1654.
[14] J. Magyar, C.E. Kiper, G. Sievert, W. Cai, G.-X. Shi, S.M. Crump, L. Li, S. Niederer, N. Smith, D.A. Andres, J. Satin, Rem-GTPase regulates cardiac myocytes L-type calcium current, Channels 6 (2012) 166–173.
[15] L. Chang, J. Zhang, Y.-H. Hseng, C.-Q. Xie, J. Ilany, J.C. Brüning, Z. Sun, X. Zhu, T. Cui, K.A. Youker, Q. Yang, S.M. Day, C.R. Kahn, Y.E. Chen, Rad GTPase deficiency leads to cardiac hypertrophy, Circulation 116 (2008) 2976–2983.
[16] R.A. Lynch, L. Wagoner, S. Li, L. Sparks, J. Molkentin, G.W. Dorn 2nd, Novel and non detected human signaling protein polymorphisms, Physiol. Genomics 10 (2002) 159–168.
[17] H. Gao, F. Wang, W. Wang, C.A. Makarewich, H. Zhang, H. Kubo, R.M. Berretta, L.A. Barr, J.D. Molkentin, S.R. Houser, Ca^{2+} influx through L-type Ca^{2+} channels and transient receptor potential channels activates pathological hypertrophy signaling, J. Mol. Cell. Cardiol. 53 (2012) 657–667.
[18] A. Mikami, K. Imoto, T. Tanabe, T. Niidome, Y. Mori, H. Takeshima, S. Narumiya, S. Numa, Primary structure and functional expression of the cardiac dihydropyridine-sensitive calcium channel, Nature 340 (1989) 230–233.
[19] W. Xu, D. Lipscombe, Neuronal $Ca_V1.3\alpha1$ L-type channels activate at relatively hyperpolarized membrane potentials and are incompletely inhibited by dihydropyridines, J. Neurosci. 21 (2001) 5944–5951.
[20] H.L. Kim, H. Kim, P. Lee, R.G. King, H. Chin, Rat brain expresses an alternatively spliced form of the dihydropyridine-sensitive L-type calcium channel α_2 subunit, Proc. Natl. Acad. Sci. USA 89 (1992) 3251–3255.
[21] E. Perez-Reyes, A. Castellano, H.S. Kim, P. Bertrand, E. Baggstrom, A.E. Lacerda, X.Y. Wei, L. Birnbaumer L, Cloning and expression of a cardiac/brain beta subunit of the L-type calcium channel, J. Biol. Chem. 267 (1992) 1792–1797.
[22] J.O. Tellez, M. Mczewsk, J. Yanni, P. Sutyagin, U. Mackiewicz, A. Atkinson, S. Inada, A. Beresewicz, R. Billeter, H. Dobrzynski, M.R. Boyett, Ageing-dependent remodelling of ion channel and Ca^{2+} clock genes underlying sino-atrial node pacemaking, Exp. Physiol. 96 (2011) 1163–1178.
[23] C.J. Christel, N. Cardona, P. Mesirca, S. Herrmann, F. Hofmann, J. Striessnig, A. Ludwig, M.E. Mangoni, A. Lee, Distinct localization and modulation of $Ca_V1.2$ and $Ca_V1.3$ L-type Ca^{2+} channels in mouse sinoatrial node, J. Physiol. 590 (2012) 6327–6342.
[24] N. Hagiwara, H. Irisawa, M. Kameyama, Contribution of two types of calcium currents to the pacemaker potentials of rabbit sino-atrial node cells, J. Physiol. 395 (1988) 233–253.
[25] E.E. Verheijck, A.C. van Ginneken, R. Wilders, L.N. Bouman, Contribution of L-type Ca^{2+} current to electrical activity in sinoatrial nodal myocytes of rabbits, Am. J. Physiol. 276 (1999) H1064–H1077.
[26] J. Platzer, J. Engel, A. Schrott-Fischer, K. Stephan, S. Bova, H. Chen, H. Zheng, J. Striessnig, Congenital deafness and sinoatrial node dysfunction in mice lacking class D L-type Ca^{2+} channels, Cell 102 (2000) 89–97.
[27] M.E. Mangoni, B. Couette, E. Bourinet, J. Platzer, D. Reimer, J. Striessnig, J. Nargeot, Functional role of L-type $Ca_V1.3$ Ca^{2+} channels in cardiac pacemaker activity, Proc. Natl. Acad. Sci. USA 100 (2003) 5543–5548.
[28] S.M. Baig, A. Koschak, A. Lieb, M. Gebhart, C. Dafinger, G. Nürnberg, A. Ali, I. Ahmad, M.J. Sinnegger-Brauns, N. Brandt, J. Engel, M.E. Mangoni, M. Farooq, H.U. Khan, P. Nürnberg, J. Striessnig, H.J. Bolz, Loss of $Ca_V1.3$ (*CACNA1D*) function in a human channelopathy with bradycardia and congenital deafness, Nat. Neurosci. 14 (2011) 77–84.
[29] J.S. Caldwell, J.S. Moyer, A. Doria, C. Reynet, C.R. Kahn, Molecular cloning of the human Rad gene: gene structure and complete nucleotide sequence, Biochim. Biophys. Acta 1316 (1996) 145–148.
[30] B.S. Finlin, D.A. Andres, Rem is a new member of the Rad- and Gem/Kir Ras-related GTP-binding protein family repressed by lipopolysaccharide stimulation, J. Biol. Chem. 272 (1997) 21982–21988.
[31] H. Chen, H.L. Puhl, S.-L. Niu, D.C. Mitchell, S.R. Ikeda, Expression of Rem2, an RGK family small GTPase, reduces N-type calcium current without affecting channel surface density, J. Neurosci. 25 (2005) 9762–9772.
[32] R.N. Correll, C. Pang, B.S. Finlin, A.M. Dailey, J. Satin, D.A. Andres, Plasma membrane targeting is essential for Rem-mediated Ca^{2+} channel inhibition, J. Biol. Chem. 282 (2007) 28431–28440.
[33] R. Flynn, L. Chen, S. Hameed, J.D. Spafford, G.W. Zamponi, Molecular determinants of Rem2 regulation of N-type calcium channels, Biochem. Biophys. Res. Commun. 368 (2008) 827–831.
[34] P. Béguin, R.N. Mahalakshmi, K. Nagashima, D.H. Cher, H. Ikeda, Y. Seino, W. Hunziker, Nuclear sequestration of beta-subunits by Rad and Rem is controlled by 14-3-3 and calmodulin and reveals a novel mechanism for Ca^{2+} channel regulation, J. Mol. Biol. 355 (2006) 34–46.
[35] Y. Ward, B. Spinelli, M.J. Quon, H. Chen, S.R. Ikeda, K. Kelly, Phosphorylation of critical serine residues in Gem separates cytoskeletal reorganization from down-regulation of calcium channel activity, Mol. Cell. Biol. 24 (2004) 651–661.
[36] K. Kelly, The RGK family: a regulatory tail of small GTP-binding proteins, Trends Cell Biol. 15 (2005) 640–643.
[37] R.N. Correll, C. Pang, D.M. Niedowicz, B.S. Finlin, D.A. Andres, The RGK family of GTP-binding proteins: regulators of voltage-dependent calcium channels and cytoskeleton remodeling, Cell. Signal. 20 (2008) 292–300.
[38] J.S. Moyers, P.J. Bilan, C. Reynet, C.R. Kahn, Overexpression of Rad inhibits glucose uptake in cultured muscle and fat cells, J. Biol. Chem. 271 (1996) 23111–23116.
[39] J. Ilany, P.J. Bilan, S. Kapur, J.S. Caldwell, M.E. Patti, A. Marette, C.R. Kahn, Overexpression of Rad in muscle worsens diet-induced insulin resistance and glucose intolerance and lowers plasma triglyceride level, Proc. Natl. Acad. Sci. USA 103 (2006) 4481–4486.
[40] Z. Sun, J. Zhang, J. Zhang, C. Chen, Q. Du, L. Chang, C. Cao, M. Zheng, M.T. Garcia-Barrio, Y.E. Chen, R.P. Xiao, J. Mao, X. Zhu, Rad GTPase induces cardiomyocyte apoptosis through the activation of p38 mitogen-activated protein kinase, Biochem. Biophys. Res. Commun. 409 (2011) 52–57.
[41] J. Zhang, L. Chang, C. Chen, M. Zhang, Y. Luo, M. Hamblin, L. Villacorta, J.W. Xiong, Y.E. Chen, J. Zhang, X. Zhu, Rad GTPase inhibits cardiac fibrosis through connective tissue growth factor, Cardiovasc. Res. 91 (2011) 90–98.